Shears mechanism in ^{109}In

D. Negi,[1,2,*] T. Trivedi,[3] A. Dhal,[1,9] S. Kumar,[4] V. Kumar,[4] S. Roy,[5] M. K. Raju,[6] S. Appannababu,[1,7] G. Mohanto,[1] J. Kaur,[8] R. K. Sinha,[9] D. Choudhury,[10] D. Singh,[1] R. Kumar,[1] R. P. Singh,[1] S. Muralithar,[1] A. K. Bhati,[8] S. C. Pancholi,[1,4] and R. K. Bhowmik[1]

[1]*Inter University Accelerator Centre, Aruna Asaf Ali Marg, New Delhi 110067, India*
[2]*iThemba LABS, P.O. Box 722, Somerset West 7129, South Africa*
[3]*Department of Nuclear and Atomic Physics, Tata Institute of Fundamental Research, Mumbai 400005, India*
[4]*Department of Physics and Astrophysics, University of Delhi, Delhi 110007, India*
[5]*S.N. Bose National Centre for Basic Sciences, Block JD, Sector III, Kolkata 700098, India*
[6]*Department of Nuclear Physics, Andhra University, Visakhapatnam 530003, India*
[7]*Department of Physics, M.S. University of Baroda, Vadodara 390002, India*
[8]*Department of Physics, Punjab University, Chandigarh 160014, India*
[9]*Department of Physics, Banaras Hindu University, Varanasi 221005, India*
[10]*Department of Physics, Indian Institute of Technology, Roorkee 247667, India*

(Received 13 December 2011; revised manuscript received 20 April 2012; published 16 May 2012)

High spin states of ^{109}In were investigated using the reaction ^{96}Zr(^{19}F, 6n)^{109}In at a beam energy of 105 MeV. New level sequences have been found in this nucleus. In an earlier known band, the ordering of some of the transitions have been changed and assigned a three-quasiparticle $\pi(g_{9/2})^{-1} \otimes \nu[h_{11/2}(d_{5/2}/g_{7/2})]$ configuration. Similar three-quasiparticle bands have also been found earlier in lighter mass ^{105}In and ^{107}In nuclei. Systematics of these bands in ^{105}In, ^{107}In, and ^{109}In nuclei are discussed in the present work within the framework of the tilted axis cranking model.

DOI: 10.1103/PhysRevC.85.057301 PACS number(s): 21.10.Hw, 21.10.Re, 21.60.−n, 23.20.−g

Nuclei in the mass $A \sim 110$ region have been the focus of study in recent years for the investigation of the phenomenon of magnetic rotation [1–8]. Being in close vicinity of the $Z = 50$ shell closure, these nuclei have low deformation ($\epsilon \sim 0.1$) and therefore the observation of rotation-like structures, with $\Delta I = 1$ $M1$ transitions, requires an alternative interpretation. These were explained in terms of the shears mechanism within the framework of the tilted axis cranking (TAC) model [9], where spins and excitation energies in a nucleus are generated by the gradual alignment of valence neutrons $\mathbf{j}_\nu$ and protons $\mathbf{j}_\pi$ spin vectors toward the total angular momentum vector $\mathbf{I}$. The bandhead state is formed by the perpendicular coupling of $\mathbf{j}_\nu$ and $\mathbf{j}_\pi$, which results in an angle θ of $\mathbf{I}$ with respect to the symmetry axis. In this mass region the configuration of these bands involve the participation of low-Ω $h_{11/2}$ and $d_{5/2}$ or $g_{7/2}$ neutron particles that are aligned along the rotation axis and high-Ω $g_{9/2}$ proton holes, which are aligned along the symmetry axis. Recently in ^{107}In, a $\Delta I = 1$ $M1$ dipole band built on a three-quasiparticle configuration (3-qp) has been identified as a magnetic rotational band [10]. The contribution from the collective rotation was found to be quite small ($\epsilon = 0.08$ from TAC calculations). An interesting question arises as to how this contribution from collective rotation changes for the same quasiparticle configuration along an isotopic chain. This is the subject of the present work.

In this work, high spin states of ^{109}In were populated using the reaction ^{96}Zr(^{19}F, 6n)^{109}In at a beam energy of 105 MeV delivered by the 15UD Pelletron Accelerator at the Inter University Accelerator Centre (IUAC), New Delhi [11]. The γ rays emitted in the reaction were detected by the Indian National Gamma Array (INGA) [12], which at the time of experiment was comprised of 14 Compton-suppressed Ge clover detectors with two at 32°, two at 57°, four at 90°, two at 123°, and four at 148° with respect to the beam axis. An isotopically enriched ^{96}Zr target of thickness 1.0 mg/cm^2 with 10.0-mg/cm^2-thick natural Pb backing was used. The data acquisition and analysis procedure is the same as explained by the authors of Ref. [10].

The level scheme proposed for ^{109}In is shown in Fig. 1. The previous level scheme [13,14] has been modified and extended. This includes the observation of bands 2 and 5 for the first time and reordering of the placement of some of the transitions in bands 1 and 4. The properties of the transitions extracted are listed in Table I. Multipolarities of the transitions were determined using the directional correlation from oriented nuclei (DCO) measurements and the results are tabulated in Table I. The results of DCO measurements are in agreement with those found in Refs. [13,14] and therefore the $\mathbf{I}^\pi$ assignments, except for band 4, have been adopted from these references.

Band 1 was observed earlier in the work done by Kownacki *et al.* [13]. They placed the 589-keV transition at the top of this band. In the present work, this transition was not found in coincidence with other transitions of band 1 (except for the 555-keV transition) above $25/2^-$. Rather, a new sequence of transitions of energies 589 and 555 keV (labeled as band 2) decaying via a 636-keV transition to the $25/2^-$ level of band 1 was observed. A linking transition of energy 396 keV [$29/2^{(-)} \to 27/2^{(-)}$] between bands 1 and 2 was also observed. The DCO ratios of the transitions of bands 1 and 2 suggest their dipole nature (see Table I).

*din_physics@yahoo.co.in

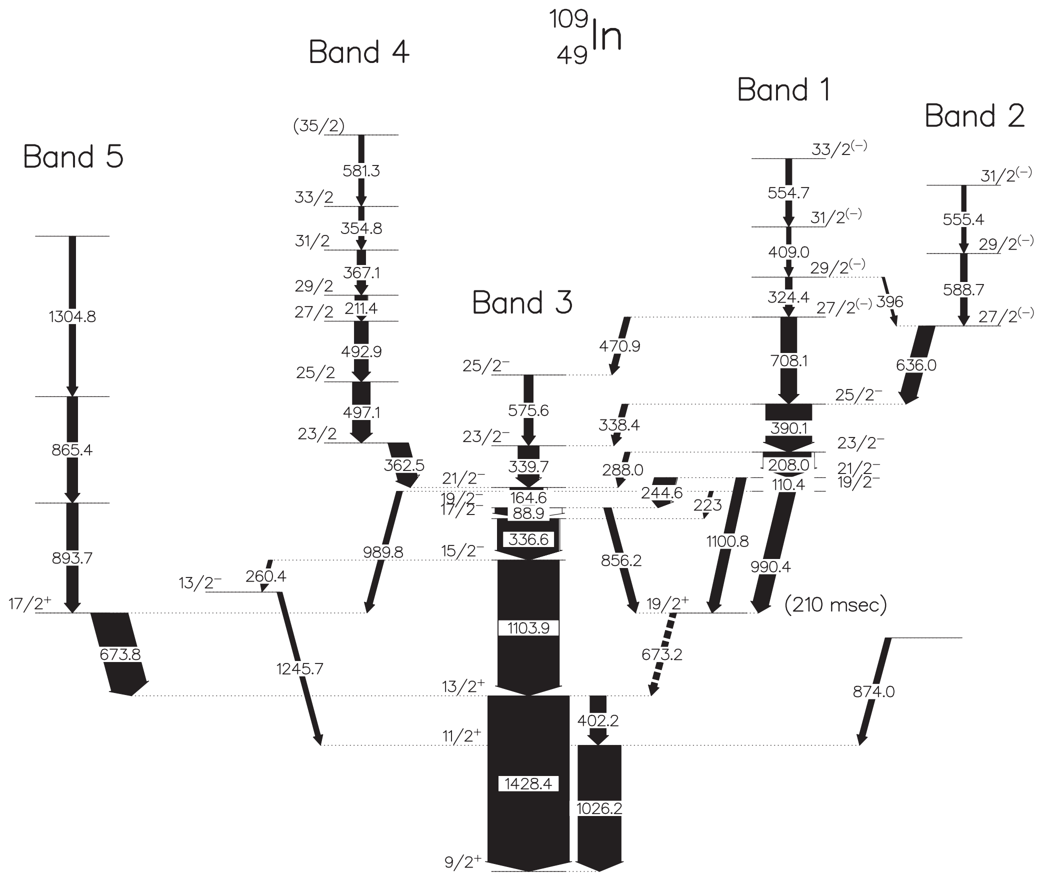

FIG. 1. Level scheme of ^{109}In deduced from the present data. The width of each arrow is proportional to the intensity of transition.

Another modification in this work in comparison to earlier works [13,14] is the change in intensities of transitions in bands 1 and 2. It was observed that the intensities of 990- and 1101-keV transitions decaying from the $19/2^-$ and $21/2^-$ level of band 1 to the $19/2^+$, 210 ms isomeric level at 2102-keV excitation energy, are significantly higher than reported in Ref. [14]. This isomeric level then decays to the $13/2^+$ level via a 674-keV transition (Ref. [14]). Whereas in Ref. [13], these transitions were not observed, instead a 990-keV transition was reported to decay to a prompt level at 2102 keV which also decays through a 674-keV transition. As a consequence, the work of the authors of Ref. [13] also does not reflect the loss in intensities of the transitions of band 1 due to its decay to the isomeric level. Although the prompt 674-keV transition was also observed in the work of Ref. [14] it was not placed in the level scheme. In the present work, band 1 is observed to decay to both the levels at 2102 keV. This is verified in the gate of the 110-keV transition (see Fig. 2), where the coincidence between the 110- and 674-keV transitions is observed, thereby suggesting the decay of band 1 to the prompt level. Whereas a relatively large intensity of the 990-keV transition in comparison to the intensity of the 674-keV transition suggest the decay to the isomeric level. Further, the observed coincidence between the 674- and 894-keV transitions corroborate the existence of prompt level (see inset of Fig. 2). These results also suggest the existence of two transitions of nearly the same energy of 990-keV decaying from the $19/2^-$ level to both the isomeric and the prompt level. The relative intensities of these transitions were then found from the 110-keV gated spectrum (see Fig. 2), where the intensity of the 674-keV transition was observed to be significantly lower (about one-fourth) than the intensity of the 990-keV transition. This suggests that the transition having higher intensity decays to the isomeric level while the one with lesser intensity decays to the prompt level. The normalized intensities of 990- and 1104-keV transitions were then obtained from 208- and 110-keV gated spectra, respectively, where the intensities of 223- and 245-keV transitions were taken as a reference. Due to the feeding of the 990- and 1101-keV transitions to the isomeric level, the intensities of transitions for bands 1 and 2 cannot be calculated from the 1428-keV gate alone. Their intensities, therefore, were obtained from a sum spectrum of 1428-, 1101-, and a weighted 990-keV gate. The linear polarization of the 208- and 390-keV transitions of band 1 and the linking 245-keV transition were determined by the authors of Ref. [14]. In the present work, the multipolarities of the transitions of bands 1 and 2 have been determined to be dipole. From these results, the transitions of the bands 1 and 2 are assigned to be $M1$ in nature.

Band 4 was observed in the work of Ref. [13]. In the present work, based on intensity and coincidence arguments, the placement of transitions in the band has been altered. In Ref. [13], the 151- and 482-keV transitions were placed in the band. In the present work, these transitions were not observed

TABLE I. Energies, intensities, DCO ratios, and the initial and final state spins of the transitions of ^{109}In deduced in the present work. Q and D stand for the quadrupole and dipole natures of the gated transition.

E_γ (keV)	E_x (keV)	I_γ	$R_{\mathrm{DCO}}(Q)$	$R_{\mathrm{DCO}}(D)$	$J_i^\pi \rightarrow J_f^\pi$
88.9	2957.8	63.6(42)			$\frac{19}{2}^- \rightarrow \frac{17}{2}^-$
110.4	3202.4	31.2(19)		0.99(21)	$\frac{21}{2}^- \rightarrow \frac{19}{2}^-$
164.6	3122.4	54.2(25)	0.78(8)		$\frac{21}{2}^- \rightarrow \frac{19}{2}^-$
208.0	3410.4	78.2(41)	0.75(14)		$\frac{23}{2}^- \rightarrow \frac{21}{2}^-$
211.4	4686.3	19.9(12)	0.56(17)	1.15(20)	$\frac{29}{2} \rightarrow \frac{27}{2}$
223.1	3092.0	6.0(15)			$\frac{19}{2}^- \rightarrow \frac{17}{2}^-$
244.6	3202.4	35.2(17)	0.70(10)		$\frac{21}{2}^- \rightarrow \frac{19}{2}^-$
260.4	2532.3	6.6(7)			$\frac{15}{2}^- \rightarrow \frac{13}{2}^-$
288.0	3410.4	8.4(10)		1.00(28)	$\frac{23}{2}^- \rightarrow \frac{21}{2}^-$
324.4	4833.0	23.6(12)	0.73(18)		$\frac{29}{2}^{(-)} \rightarrow \frac{27}{2}^{(-)}$
336.6	2868.9	99.8(41)	0.69(4)		$\frac{17}{2}^- \rightarrow \frac{15}{2}^-$
338.4	3800.5	9.7(13)	0.56(5)[a]		$\frac{25}{2}^- \rightarrow \frac{23}{2}^-$
339.7	3800.5	33.9(38)	0.56(5)[a]		$\frac{23}{2}^- \rightarrow \frac{21}{2}^-$
354.8	5408.2	8.8(9)		1.18(37)	$\frac{33}{2} \rightarrow \frac{31}{2}$
362.5	3484.9	32.6(13)	0.63(10)		$\frac{23}{2} \rightarrow \frac{21}{2}^-$
367.1	5053.4	13.8(9)		1.00(28)	$\frac{31}{2} \rightarrow \frac{29}{2}$
390.1	3800.5	74.1(39)	0.61(8)		$\frac{25}{2}^- \rightarrow \frac{23}{2}^-$
396.5	4833.0	4.0(5)			$\frac{29}{2}^{(-)} \rightarrow \frac{27}{2}^{(-)}$
402.2	1428.4	26.0(18)			$\frac{13}{2}^+ \rightarrow \frac{11}{2}^+$
409.0	5242.0	16.4(10)		1.19(23)	$\frac{31}{2}^{(-)} \rightarrow \frac{29}{2}^{(-)}$
470.9	4508.6	9.9(10)		0.93(14)	$\frac{27}{2}^{(-)} \rightarrow \frac{25}{2}^-$
492.9	4474.9	22.6(13)		1.20(22)	$\frac{25}{2} \rightarrow \frac{23}{2}$
497.2	3982.0	28.7(15)		1.03(16)	$\frac{27}{2} \rightarrow \frac{25}{2}$
555.4	5580.6	7.4(12)		0.94(33)[b]	$\frac{31}{2}^{(-)} \rightarrow \frac{29}{2}^{(-)}$
554.7	5796.7	3.1(15)		0.94(33)[b]	$\frac{33}{2}^{(-)} \rightarrow \frac{31}{2}^{(-)}$
575.6	4037.7	14.8(8)		1.04(17)	$\frac{25}{2}^- \rightarrow \frac{23}{2}^-$
581.3	5989.5	8.8(9)		1.11(38)	$(\frac{35}{2}) \rightarrow \frac{33}{2}$
588.7	5025.2	11.0(10)		1.03(46)	$\frac{29}{2}^{(-)} \rightarrow \frac{27}{2}^{(-)}$
636.0	4436.5	26.0(13)		0.97(21)	$\frac{27}{2}^{(-)} \rightarrow \frac{25}{2}^-$
673.2[c]	2101.6				$\frac{19}{2}^+ \rightarrow \frac{13}{2}^+$
673.8	2102.2	58.6(27)	1.13(14)		$\frac{17}{2}^+ \rightarrow \frac{13}{2}^+$
708.1	4508.6	24.4(9)		1.28(19)	$\frac{27}{2}^{(-)} \rightarrow \frac{25}{2}^-$
856.2	2868.9	12.7(8)			$\frac{19}{2}^- \rightarrow \frac{19}{2}^+$
865.4	3861.3	17.1(12)			
874.0	1900.2	9.9(8)			
893.7	2995.9	18.8(15)			$\rightarrow \frac{17}{2}^+$
989.8	3092.0	9.6(11)			$\frac{19}{2}^- \rightarrow \frac{17}{2}^+$
990.4	3092.0	26.0(47)			$\frac{19}{2}^- \rightarrow \frac{19}{2}^+$
1026.2	1026.2	69.8(29)			$\frac{11}{2}^+ \rightarrow \frac{9}{2}^+$
1100.8	3202.4	16.5(8)			$\frac{21}{2}^- \rightarrow \frac{19}{2}^+$
1103.8	2532.3	100.0	0.50(5)		$\frac{15}{2}^- \rightarrow \frac{13}{2}^+$
1245.7	2271.9	8.3(8)			$\frac{13}{2}^- \rightarrow \frac{11}{2}^+$
1304.8	5166.1	10.6(11)			
1428.4	1428.4	132.6(81)			$\frac{13}{2}^+ \rightarrow \frac{9}{2}^+$

[a]Determined for the combined 338.4- and 339.7-keV transitions.
[b]Determined for the combined 554.7- and 555.4-keV transitions.
[c]Delayed transition not observed in the present work.

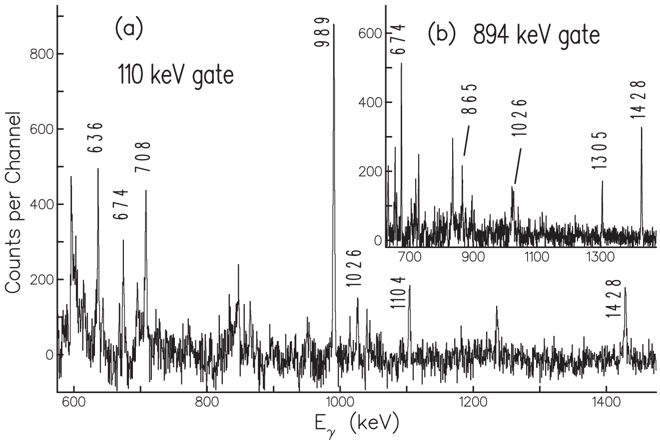

FIG. 2. γ-ray energy spectrum gated by the (a) 110-keV and (b) 894-keV transitions in bands 1 and 5, respectively.

in coincidence with the transitions of the band. The 211-keV transition, which was placed in an anticoincidence relationship with the 362-keV transition in Ref. [13], has been observed to be in coincidence with the 362-keV transition. The decay out 362 keV and all the other in-band transitions have been found to be of a dipole nature. A new sequence of transitions of energies 894, 865, and 1305 keV on top of the $17/2^+$ level at 2102-keV excitation energy has been observed. The sequence is labeled as band 5.

A sequence similar to band 1 was observed in ^{107}In (band 1 in Ref. [10]) and ^{105}In [13,15], where the configuration $\pi(g_{9/2})^{-1} \otimes \nu[h_{11/2}(d_{5/2}/g_{7/2})]$ has been assigned for the sequence before the alignment of pair of neutrons in $(d_{5/2}/g_{7/2})$. In the upper panel of Fig. 3, the observed spins I as a function of rotational frequency $\hbar\omega$ for band 1 of ^{105}In, ^{107}In, and ^{109}In are plotted. The similar behavior of the plots, especially the frequency of the band crossing at about 0.43 MeV and the alignment gain of about $4.5\hbar$ at the crossing frequency, suggests similar configurations for all three bands, both before and after the alignment.

In our earlier work [10], it was established that the shears mechanism is the dominant mode of excitation in band 1 of ^{107}In. Band 1 of ^{109}In, therefore, was analyzed in light of this phenomenon. The TAC calculations have been carried out for configurations mentioned in the previous paragraph and were compared with the experimental results for this band (lower panel of Fig. 3). In these calculations, the values of the proton paring gap parameter $\Delta_\pi = 0.99$ MeV and the neutron pairing gap parameter $\Delta_\nu = 0.85$ MeV were used. These values are 0.6 and 0.8 times the odd-even mass difference, respectively. The chemical potential λ_ν was chosen to reproduce the particle number of $N = 60$. The deformation parameters ϵ_2 and γ used were obtained from the Nilsson Strutinsky's minimization procedure. These values were found to be $\epsilon_2 = 0.15$, $\gamma = 9^\circ$ for the states before the alignment and $\epsilon_2 = 0.08$, $\gamma = 20^\circ$ after the alignment. Good agreement between the calculations and experimental results is obtained. However, in Ref. [10], it was shown for the similar band in ^{107}In that the agreement between the calculations and experimental results for the states before the neutron alignment were better for the calculations performed with lower deformation values than the value obtained from the minimization procedure. This conclusion was also supported by the observation of a rapid decrease in $B(M1)$ strength with increase in spin, thereby indicating a very small contribution from the core toward the angular momentum generation. Therefore, the calculations for these states in ^{109}In before the alignment were performed with a lower deformation value of $\epsilon_2 = 0.08$ obtained by reducing the strength of the coupling constant of the quadrupole-quadrupole (QQ) interaction. The result shows an improvement in the agreement. Comparing this result with the one obtained for the same configuration in ^{107}In (band 1 before the neutron alignment) indicates that there is no significant change in the deformation of the states when going from $N = 58$ to $N = 60$. In other words, there is no significant change in the contribution from the core toward the total angular momentum when going from $N = 58$ to $N = 60$. The result can be explained by the observation that the extra pair of neutrons in ^{109}In are in the $(d_{5/2}/g_{7/2})$ orbitals, which do not drive the nucleus toward strong deformation.

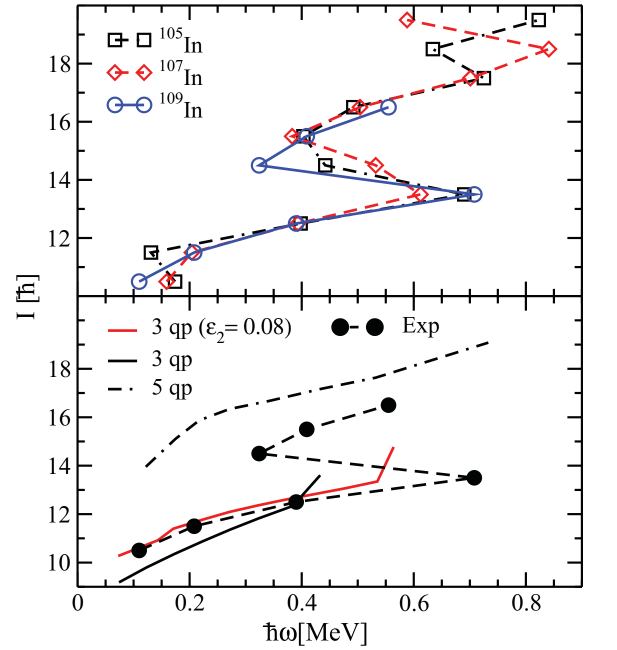

FIG. 3. (Color online) Plot of angular momentum I as a function of rotational frequency $\hbar\omega$ for band 1 in ^{105}In, ^{107}In, and ^{109}In (upper panel). In the lower panel a comparison with the TAC calculations is shown for the band in ^{109}In. 3qp stands for calculations for the three-quasiparticle configuration $\pi(g_{9/2})^{-1}\otimes\nu[h_{11/2},(d_{7/2}/g_{7/2})]$ of the band before alignment. Similarly, 5qp stands for calculations for five-quasiparticle configuration $\pi(g_{9/2})^{-1}\otimes\nu[h_{11/2},(d_{7/2}/g_{7/2})^3]$ of the band after the alignment. Also shown is the comparison with calculations done with the lower deformation value of $\epsilon_2 = 0.08$ for 3qp configuration.

In the present work, we compared the relative contribution of the core and the shears mechanism for a particular set of quasiparticle configuration in ^{107}In and ^{109}In. The results indicate that this relative contribution does not significantly change when going from $N = 56$ to $N = 60$.

We would like to thank the staff of the 15UD Pelletron and target laboratory at IUAC, the INGA collaboration, and the Department of Science and Technology, India, for providing funds for the INGA project (No. IR/S2/PF-03/2003-I). D.N. would like to acknowledge CSIR, India, for financial assistance.

[1] A. Gadea *et al.*, Phys. Rev. C **55**, R1 (1997).
[2] P. Vaska *et al.*, Phys. Rev. C **57**, 1634 (1998).
[3] D. G. Jenkins *et al.*, Phys. Rev. Lett. **83**, 500 (1999).
[4] C. J. Chiara *et al.*, Phys. Rev. C **64**, 054314 (2001).
[5] P. Datta *et al.*, Phys. Rev. C **67**, 014325 (2003).
[6] A. Deo *et al.*, Phys. Rev. C **73**, 034313 (2006).
[7] S. Roy *et al.*, Phys. Lett. B **694**, 322 (2011).
[8] S. Roy *et al.*, Phys. Rev. C **81**, 054311 (2010).
[9] S. Frauendorf, Rev. Mod. Phys. **73**, 463 (2001).
[10] D. Negi *et al.*, Phys. Rev. C **81**, 054322 (2010).
[11] G. K. Mehta and A. P. Patro, Nucl. Instrum. Methods Phys. Res. **268**, 334 (1988).
[12] S. Muralithar *et al.*, Nucl. Instrum. Methods A **622**, 281 (2010).
[13] J. Kownacki *et al.*, Nucl. Phys. A **627**, 239 (1997).
[14] A. Van Poelgeest, W. H. A. Heeselink, J. Bron, J. J. A. Zalmstra, M. J. Uttzinger, and H. Verheul, Nucl. Phys. A **327**, 12 (1979).
[15] G. de Angelis *et al.*, Nucl. Phys. A **654**, 659c (1999).